The ^{3}He Abundance in the Planetary Nebula NGC 3242

Dana S. Balser[1], Robert T. Rood[2], and T. M. Bania[3]

ABSTRACT

Using the NRAO 140 Foot radio telescope we have confirmed our earlier detection of ^{3}He in the planetary nebula NGC 3242 made with the 100 m radio telescope of the MPIfR. Both spectrometers show that the observed ^{3}He$^+$ hyperfine line has a double peaked structure. This line shape naturally arises if NGC 3242 is modeled as a dense core surrounded by a very low density expanding shell. The observed ^{3}He$^+$ emission suggests an abundance by number of ^{3}He/H = 2–5 $\times 10^{-4}$ which is more than an order of magnitude higher than typically found in Galactic H II regions.

Subject headings: planetary nebulae – ISM: abundances – nuclear reactions, nucleosynthesis, abundances – radio lines: ISM

1. Introduction

The light element ^{3}He is produced in significant amounts during the era of primordial nucleosynthesis (e.g., Yang et al. 1984). This cosmological abundance is then altered by stellar nucleosynthesis over many generations of star formation and evolution in the Galaxy. For many years stellar evolution models have predicted that low-mass stars should produce ^{3}He (e.g., Iben 1967; Vassiliadis & Wood 1993). Standard models also predict that red giant branch (RGB) and asymptotic giant branch (AGB) stellar winds, and planetary nebulae of stars with masses $M < 2\,M_\odot$ should be substantially enriched in ^{3}He (Rood, Steigman, & Tinsley 1976). If this is true then the ^{3}He/H abundance should grow with time and be higher in those parts of the Galaxy where there has been substantial stellar processing.

Measurements of ^{3}He in protosolar material (Geiss 1993), the local interstellar medium (Gloeckler & Geiss 1996), and Galactic H II regions (Balser et al. 1999; hereafter BBRW99) all indicate that the ^{3}He/H abundance ratio is $\sim 2 \times 10^{-5}$ by number. The H II regions are expected to be zero-age objects, yet there is no evidence for *any* stellar ^{3}He enrichment during the last 4.5 Gyr (Rood et al. 1998). Observations of the ^{3}He$^+$ hyperfine line in planetary nebulae (PNs) were made using the Max-Planck-Institut für Radioastronomie (MPIfR) 100 m telescope. A small survey of 6 PNs produced a detection in NGC 3242 (Rood, Bania, & Wilson 1992) and probable detections in two other sources (BBRW97). These objects have enriched ^{3}He (^{3}He/H $\sim 10^{-4}$ – 10^{-3}) as predicted by standard stellar evolution models (Balser et al. 1997; hereafter BBRW97). The fact that the observed abundances of ^{3}He throughout the Galaxy disagreed so strongly with chemical

[1]National Radio Astronomy Observatory, Green Bank WV 24944

[2]Department of Astronomy, University of Virginia, Charlottesville VA 22903

[3]Astronomy Department, Boston University, Boston MA 02215

evolution models coupled with the observations that some stars do indeed produce ^{3}He led to what is called "The ^{3}He Problem" (Galli et al. 1997). This has stimulated studies of many non-standard models for both stellar and Galactic chemical evolution which deplete ^{3}He in low-mass stars (e.g., Charbonnel 1995).

The ^{3}He$^+$ observations of PNs at the MPIfR 100 m were at the instrumental sensitivity limit of this telescope. Because of the importance of these observations, we have re-observed NGC 3242 using the National Radio Astronomy Observatory (NRAO)[4] 140 Foot telescope. These observations provide an independent confirmation that at least this one object enriches the interstellar ^{3}He abundance. The observations made at the 140 Foot are described in §2. In §3 we describe the models used to derive the ^{3}He/H abundance ratio. The implications of these results are discussed in §4.

2. NRAO 140 Foot Telescope Observations

These observations were part of a larger project at Green Bank to measure the ^{3}He abundance in the Galaxy primarily using H II regions (Bania et al. 1997; hereafter BBRWW97). Traditionally we have observed H II regions with the 140 Foot telescope since any ^{3}He$^+$ emission from the small angular sized PNs (< 1 arcmin) will be diluted within the 3.2 arcmin half-power beamwidth (HPBW) of the 140 Foot. Nevertheless, the importance of the ^{3}He abundance in NGC 3242 demanded that we attempt to confirm its abundance with the 140 Foot telescope. This observation is feasible because NGC 3242 appears to have a very large halo which would fill the 140 Foot telescope's beam (BBRW97).

Observations of NGC 3242 with the 140 Foot telescope were made during the following periods: 1994 May, 1996 December, 1997 January, 1997 May, 1997 June, 1997 September, 1998 January, 1998 June, 1998 July, 1998 August, 1998 September, 1998 December, 1999 March, and 1999 May. The observational procedures and data reduction techniques are discussed in BBRWW97. Briefly, the X-band Cassegrain receiver was a dual polarization HFET with a system temperature of ~ 35 K. The spectrometer was an autocorrelator split into four sections, each covering a total bandwidth of 20 MHz and consisting of 256 channels, yielding a velocity resolution of 2.7 km sec^{-1} per channel. Spectra were taken using the total power observing mode with the ^{3}He$^+$ transition always in two of the four autocorrelator quadrants. The remaining two quadrants were tuned to various radio recombination lines (RRLs).

We have confirmed the detection of ^{3}He$^+$ emission in NGC 3242 using two independent spectrometer systems. The ^{3}He$^+$ spectra observed with both telescopes are shown in Figure 1. The bold curve is the main beam brightness temperature spectrum measured by the MPIfR 100 m telescope (BBRW97). The thin curve is the main beam brightness temperature spectrum measured by the 140 Foot telescope with the observed intensity multiplied by a factor of four. Both spectra show a double-peaked profile centered at the expected ^{3}He$^+$ transition frequency. The two peaks separated by $\sim$30 km sec^{-1} are caused by a systematic nebular expansion (cf., BBRW97).

---

[4]The National Radio Astronomy Observatory is a facility of the National Science Foundation operated under cooperative agreement by Associated Universities, Inc.

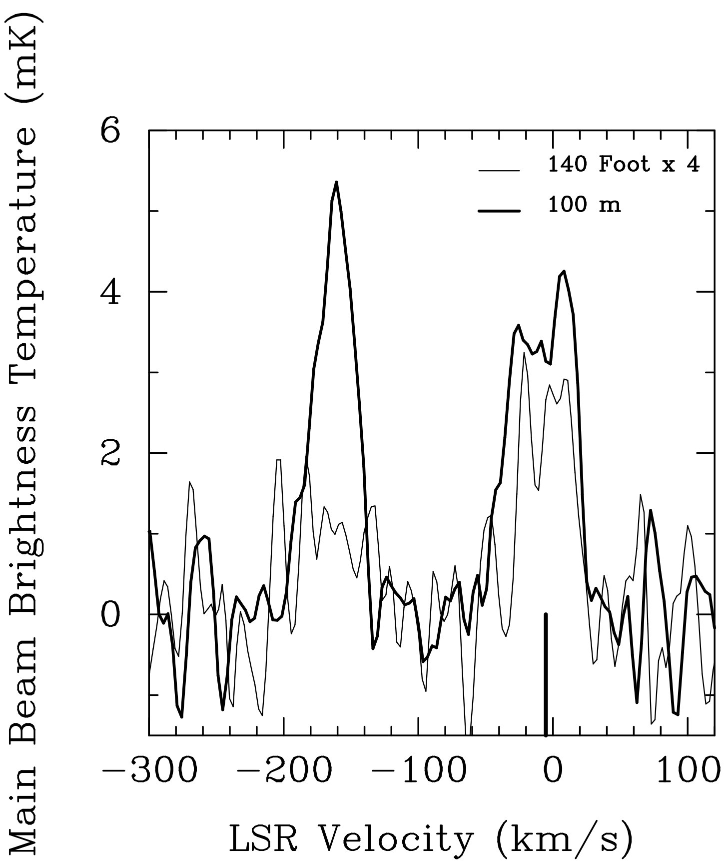

Fig. 1.— Confirmation of the detection of $^3He^+$ emission in the planetary nebula NGC 3242. The bold curve is the main beam brightness temperature spectrum measured by the MPIfR 100 m telescope. The thin curve is the main beam brightness temperature spectrum measured by the NRAO 140 Foot telescope with the observed intensity multiplied by a factor of four. For the sake of comparison here we have converted the 140 Foot data from antenna temperature to main beam brightness temperature. The vertical line at $-5.3\,\mathrm{km\,sec^{-1}}$ flags the $^3He^+$ emission at the LSR velocity of NGC 3242. The prominent feature in the MPIfR spectrum is the H171η recombination line. An instrumental baseline was removed from each spectrum and each was smoothed to a velocity resolution of $8.1\,\mathrm{km\,sec^{-1}}$.

3. Planetary Nebula Model

Deriving a $^3He/H$ abundance ratio from the observed $^3He^+$ hyperfine line parameters requires a model. We use a numerical code, NEBULA, to calculate the thermal free-free continuum, RRL, and $^3He^+$ hyperfine line emission produced by a model for NGC 3242. The details of NEBULA physics are discussed in BBRW99; how NEBULA models PNs is described in BBRW97. Briefly, the model nebulae are composed solely of hydrogen and helium. It is assumed that the $^3He^+$ line is in LTE and that its shape within each numerical cell is broadened only by Doppler motions. For the recombination lines the effects of non-LTE and pressure broadening from electron impacts are included. The numerical grid, a three-dimensional cartesian coordinate system, allows one to model a completely arbitrary density and ionization structure. Here we use NEBULA to model spherically concentric homogeneous shells with each shell having a constant expansion velocity relative to the center of the nebula.

Table 1. Properties of NGC 3242 Model

Component	Diameter (arcsec)	$n_{\rm e}$ ($\rm cm^{-3}$)	$v_{\rm exp}$ ($\rm km\,s^{-1}$)	$^4He^+/H^+$	$^4He^{++}/H^+$
Inner Shell	10–25	3,300	20	0.061	0.033
Outer Shell	25–44	1,600	20	0.085	0.006
Halo	44–960	10	15	0.090	0.000

As in BBRW97 we model NGC 3242 as a double shell nebula embedded in a faint halo. The physical parameters are summarized in Table 1. The distance is 0.42 ± 0.16 kpc from Hajian, Terzian, & Bignell (1995). Data from Barker (1985) are used to constrain the density and ionization structure of the double shell. The $20\,\rm km\,sec^{-1}$ expansion velocities of these components are taken from Weinberger (1989). The halo properties are not very well known: its size is estimated to be $960''$ (Rosado 1986; Chu et al. 1987). We assume a halo density of $10\,\rm cm^{-3}$, an expansion velocity of $15\,\rm km\,sec^{-1}$, and that the helium is all singly ionized. All components have an 11,000 K electron temperature (Barker 1985).

With the Table 1 model parameters NEBULA predicts free-free emission intensities that are consistent with the continuum data for both telescopes to within 5%. The bulk of the continuum and RRL emission is produced in the dense gas located in the double shell; the contribution from the halo to this emission is negligible. The $^3He^+$ emission, however, is produced in both the double shell and the halo. As discussed in BBRW97 this is because the continuum and RRL emission comes from regions with high emission measure whereas the $^3He^+$ emission results from the total source column density.

This $^3He^+$ sensitivity to total column density accounts for the double-peaked $^3He^+$ profile shape observed by both the 100 m and the 140 Foot . Since both telescopes have HPBW's larger than the double shell but smaller than the halo, each probes the optically thin $^3He^+$ gas in all the components of the nebula. In contrast, as can be seen in the Figure 2 example which shows the 140 Foot H91α spectrum, none of the RRLs show a double-peaked profile shape. This follows naturally from the model (cf., BBRW97).

Table 2 compares the $^3He^+$ and RRL line parameters observed by the 140 Foot with those predicted by NEBULA using the Table 1 model and assuming a ^{3}He/H abundance ratio of 1.5×10^{-4} by number. Listed for each transition are the modeled and observed line intensities (antenna temperature) and linewidths (FWHM) as well as the RMS noise and total integration time of each spectrum. The natural intensity scale of the 140 Foot is antenna temperature which can be directly related to laboratory measurements.

All modeled RRLs are well approximated as single-peaked Gaussian profiles with linewidths of $\sim 40\,\rm km\,sec^{-1}$. This is consistent with all observed RRL profiles that have high signal-to-noise ratios. The observed H91α RRL intensities are lower than expected from the model, however, by

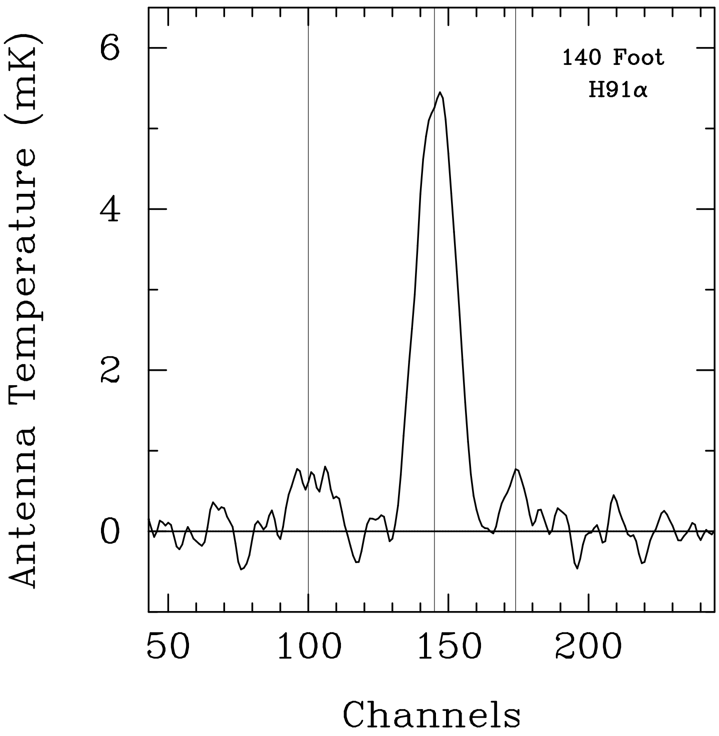

Fig. 2.— NRAO 140 Foot telescope H91α antenna temperature spectrum for NGC 3242. The horizonal axis is in channels and the LSR velocity spacing is 2.7 km sec^{-1} per channel. An instrumental baseline was removed from the spectrum and it was smoothed to a velocity resolution of 8.1 km sec^{-1}. The vertical lines flag from left to right the positions of the He91α, H91α, and H154ϵ recombination line transitions.

as much as a factor of 1.5. Although we have included non-LTE effects and pressure broadening, significant clumping of the gas could increase the local density and thus enhance the pressure broadening thereby decreasing the modeled line intensity.

A comparison between the observed and modeled ^{3}He$^+$ spectra is shown in Figure 3 for both 140 Foot and 100 m data. Note that the Figure 3 models are identical save for different values of the assumed ^{3}He/H abundance ratio. A ratio of ^{3}He/H $= 5 \times 10^{-4}$ gives a good fit to the 100 m spectrum. As noted by BBRW97, however, the observed H171η intensity is much too strong and cannot be accounted for with a simple model. An ensemble of different baseline fits to the 100 m spectrum (see Table 2 of BBBRW97) shows that the intensity of the H171η line is not well determined. The area of the line is somewhat better constrained—to a factor of two or so. Models like those in BBBRW97 can come to within a factor of two of the observed area. Still, it is clear that both better data and a more complex model are needed.

The factor of ~ 3 abundance difference required to match the two ^{3}He$^+$ spectra is not particularly disturbing. For such weak lines the observational errors, particularly those associated with modeling the 100 m spectral baseline, could account for much of the difference. Likewise, more complicated models could be devised to produce the observed ^{3}He$^+$ intensites for both data sets assuming the same ^{3}He/H abundance ratio. We conclude that a ^{3}He/H $\sim$ 2–5 $\times 10^{-4}$ abundance ratio is consistent with both observed spectra.

Table 2. NGC 3242 Spectral Line Parameters[a]

	Model		Observed			
Transition	$T_{\rm L}$ (mK)	Δv (km sec^{-1})	$T_{\rm L}$ (mK)	Δv (km sec^{-1})	rms (mK)	$t_{\rm intg}$ (hr)
^{3}He[b]	0.74	17.	0.62 ± 0.043	$10. \pm 1.0$	0.15	269.9
	0.74	17.	0.65 ± 0.024	$29. \pm 1.8$	0.15	269.9
H91α	8.6	38.	5.70 ± 0.069	$42. \pm 0.6$	0.19	247.8
He91α	0.70	35.	0.78 ± 0.074	$37. \pm 4.2$	0.19	247.8
H114β	2.4	39.	2.11 ± 0.062	$50. \pm 2.0$	0.36	83.9
H154ϵ	0.39	35.	0.74 ± 0.094	$22. \pm 3.3$	0.19	247.8
H171η	0.17	44.	—	—	0.15	269.9

[a]Gaussian fits to both modeled and observed line profiles.

[b]Double line profile fit.

Beyond this there is every reason to expect real differences in the ^{3}He$^+$ abundances in the two volumes sampled by the different telescopes. It is possible, for example, that ^{3}He is depleted during the last phase of AGB evolution. Since it probes the smaller gas volume this could diminish the 100 m line intensity relative to the 140 Foot value. On the other hand, the ^{3}He in the halo might be underionized which would weaken the line as observed with the 140 Foot which has more of the halo gas in its beam. This latter effect could give our present result since a large amount of underionized (and hence undetectable) gas would imply a neutral ^{3}He/H abundance larger than the ionized ^{3}He$^+$/H$^+$ abundance required to model the 140 Foot data.

4. Implications

The detection of ^{3}He$^+$ emission from NGC 3242 with the 140 Foot confirms our previous results with the 100 m. At least *some* low-mass stars have produced significant amounts of ^{3}He. Yet the observations of ^{3}He in zero-age H II regions imply that essentially no stellar processing has occurred over the last 4.5 Gyr (BBRW99). Chemical evolution models of the Galaxy indicate that to account for the observed abundances in H II regions 70-80% of low-mass stars must not produce ^{3}He like the progenitor of NGC 3242 (Galli et al. 1997). We emphasize that this does *not* imply that most low-mass stars must destroy their ^{3}He. The requirement is merely that ^{3}He must not be produced in significant amounts. Several studies have suggested that non-standard mixing can occur in low-mass stars during their red giant evolution (e.g., Hogan 1995). Charbonnel & do Nascimento (1998) estimate that 95% of evolved stars should go through this stage and deplete at least some of their ^{3}He. If true this could resolve "The ^{3}He Problem" and reconcile the observed ^{3}He abundances in PNs and H II regions with stellar and galactic evolution. Clearly additional observations of ^{3}He in PNs are needed.

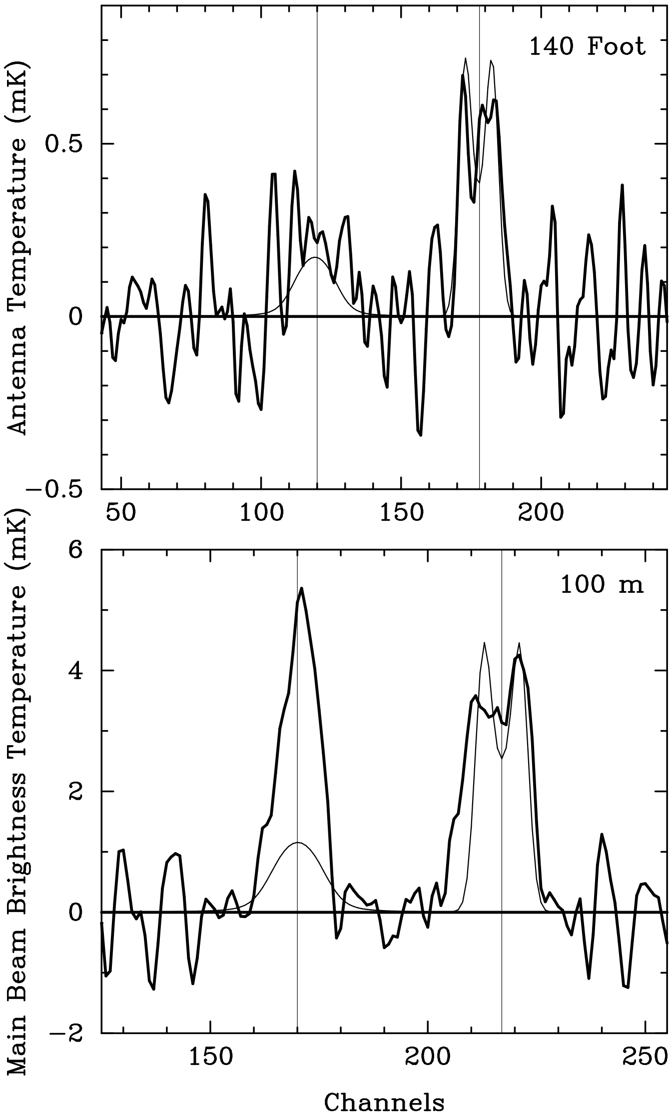

Fig. 3.— Comparison between observed and modeled spectra for $^3\mathrm{He}^+$ emission in NGC 3242. The bold curves are the Figure 1 observed spectra. The models (see text) are drawn as thin lines. The vertical lines flag from left to right the positions of the H171η and $^3\mathrm{He}^+$ transitions. *Top Panel:* NRAO 140 Foot telescope $^3\mathrm{He}^+$ antenna temperature spectrum. The model shown assumes a $^3\mathrm{He}/\mathrm{H}$ abundance ratio of 1.5×10^{-4} by number. *Bottom Panel:* MPIfR 100 m telescope $^3\mathrm{He}^+$ brightness temperature spectrum. The model shown assumes a $^3\mathrm{He}/\mathrm{H}$ abundance ratio of 5×10^{-4} by number.

We thank the international Light Elements Community for collegiality and support over the years. We thank the referee for a careful reading of the manuscript. The research was supported by a NATO Travel Grant and the National Science Foundation (AST 97-31484).

REFERENCES

Balser, D. S., Bania, T. M., Rood, R. T., & Wilson, T. L. 1997, ApJ, 483, 320 (BBRW97)

Balser, D. S., Bania, T. M., Rood, R. T., & Wilson, T. L. 1999, ApJ, 510, 759 (BBRW99)

Bania, T. M., Balser, D. S., Rood, R. T., Wilson, T. L., & Wilson, T. A. 1997, ApJS, 113, 353 (BBRWW97)

Bania, T. M., Rood, R. T., & Wilson, T. L. 1993, Max Planck Institut für Radioastronomie, Technischer Bericht, Nr. 75

Barker, T. 1985, ApJ, 294, 193

Charbonnel, C. 1995, ApJ, 453, L41

Charbonnel, C. & do Nascimento Jr, J. D. 1998, A&A, 336, 915

Chu, You-Hua, Jacoby, G. H., Arendt, R. 1987, ApJS, 64, 529

Galli, D., Stanghellini, L., Tosi, M., Palla, F. 1997, ApJ, 477, 218

Geiss, J. 1993, in Origin and Evolution of the Elements, ed. N. Prantzos, E. Vangioni-Flam, and M. Casse (Cambridge: Cambridge University Press), 89

Gloeckler, G. & Geiss, J. 1996, Nature, 381, 210

Hogan, C. J. 1995, ApJ, 441, L17

Iben, I. 1967, ApJ, 147, 650

Michaud, G., Martel, A., Montmerle, T., Cox, A. N., Magee, N. H., & Hodson, S. W. 1979, ApJ, 234, 206

Rood, R. T., Bania, T. M., & Wilson, T. L. 1992, Nature, 355, 618

Rood, R. T., Bania, T. M., Balser, D. S., & Wilson, T. L. 1998, Space Science Reviews, 84, 185

Rood, R. T., Steigman, G., & Tinsley, B. M. 1976, ApJ, 207, L57

Rosado, M. 1986, Rev. Mexicana Astron. Astrof., 13, 49

Vassiliadis, E., & Wood, P. R. 1993, ApJ, 413, 641

Weinberger, R. 1989, A&AS, 78, 301

Yang, J., Turner, M. S., Steigman, G., Schramm, D. N., & Olive, K. A. 1984, ApJ, 281, 493